Simultaneous 8- to 9-GHz and 30- to 40-GHz Feed for the Deep Space Network Large Array

D. J. Hoppe[1] and H. Reilly[1]

A dual-band feed for the Deep Space Network (DSN) large array is described. The feed covers the 8- to 9-GHz and 30- to 40-GHz bands using a coaxial configuration. A saturated corrugated horn controls the radiation pattern in the low-frequency band, and a dielectric rod is used as the radiator in the high-frequency band. The major requirements for the feed are described, and a summary of several possible feed configurations is presented. Next, the analysis tools used to perform the design are described. The bulk of the article covers the mechanical configuration of the feed, measured radiation patterns, and measured scattering parameters. Finally, the predicted performance of the feed–reflector antenna combination is presented.

I. Introduction

The Deep Space Network (DSN) is currently investigating the merits of constructing a large array of relatively small-aperture reflector antennas to meet future demands for spacecraft communication in a cost-effective manner [1]. The work is closely related to similar work in the radio astronomy community, where an array encompassing one square kilometer of collecting area, the Square Kilometer Array (SKA), is currently under investigation [2]. A large array appears to offer cost advantages over a single large-aperture reflector antenna. These cost savings stem from the advantages of mass production of the individual elements and the decreasing cost of the combining electronics as a function of time, following Moore's Law [3]. Such an array also provides increased flexibility since it may be partitioned and used in a sub-array configuration to track multiple spacecraft simultaneously. The array concept also provides a soft-failure mode wherein the loss of even several individual array elements does not result in a total loss of the spacecraft communication link.

As a first step, a breadboard array consisting of three 6-meter dual-reflector antennas is currently under construction. The breadboard array will be used to develop the technology required for the DSN large array, consisting of hundreds of antennas with diameters up to 12 meters, and to provide accurate performance and cost estimates for the large array.

---

[1] Communications Ground Systems Section.

The research described in this publication was carried out by the Jet Propulsion Laboratory, California Institute of Technology, under a contract with the National Aeronautics and Space Administration.

This article describes the design and testing of the dual-band microwave feed for these antennas. Details of the reflector antenna design and cryogenic package will be subjects of future articles. The article begins with a description of the requirements for the feed as well as a study that examined the merits of several different configurations. The design tools used in the development of the feed then are described. Mechanical and electrical details of the final feed configuration and measured data make up the bulk of the article. A short section describing the performance of the feed on the dual-reflector antenna also is included although this information will be covered in greater detail in a future article on the antenna. Future plans for slight modifications to the design that may enable a more cost-effective, mass-producible feed also are described.

II. Requirements

The major requirements for the feed are described in Table 1. Four separate bandwidths are specified, two in the DSN frequency range and two usable frequency ranges in both the X- and Ka-bands. The usable X-band range is intended to cover not only the DSN receive band but also the very long baseline interferometry (VLBI) band as well. At Ka-band, the Human Exploration of Deep Space (HEDS) receive band near 38 GHz is covered as well as the standard DSN receive band. The DSN uplink frequencies are not covered at X-band but are covered at Ka-band; however, there are no plans to transmit from the array in either band. Including the additional frequency coverage in the feed design will allow the final array to be a much more versatile instrument, allowing VLBI and radio astronomy observation as well as spacecraft communication.

Polarization for the feed is simultaneous right-hand and left-hand circular polarization in both bands. Ellipticity is specified over only the DSN communication bands and the HEDS band, where the requirement is for ellipticity of better than 0.75 dB. The return loss is specified to be better than −20 dB over both usable bands. Finally, the illumination of the feed is specified at −12 dB at an angle of 42 deg relative to the on-axis value. The illumination angle was driven by the original desire to use this feed with the existing offset Allen Telescope Array (ATA) reflector.[2] Further developments have led the DSN array project to design and fabricate its own symmetric dual-shaped reflector. This reflector was designed to operate efficiently with the existing feed illumination angle, as described in Table 1, and will be described in a future article.

Table 1. Feed requirements.

Requirement set	X-band	Ka-band
DSN band	8.4–8.5 GHz	31.8–32.3 GHz
Usable band	8.0–8.8 GHz	30.0–40.0 GHz
Polarization	Dual circular	Dual circular
Ellipticity	<0.75 dB (DSN band)	<0.75 dB (DSN Band + 37–38 GHz)
Return loss	>20 dB, usable band	>20 dB, usable band
Illumination	−12 dB at ±42 deg	−12 dB at ±42 deg

[2] W. J. Welch, "An Offset Gregorian Optical System for the Allen Telescope Array," ATA Memorandum No. 25 (internal document), Allen Telescope Array, August 10, 2000.

III. Configuration Study

The first step in the development of the feed was to examine a number of options for the design. In some cases, a preliminary design or layout was completed. In other cases, a literature search was conducted, and specifications of existing designs were compared with the requirements for this feed. Four candidate configurations emerged as best choices for the breadboard array feed. In this section, a brief description of these options is presented and the rationale for the selected approach is reviewed.

The first configuration considered is based on using a frequency-selective surface (FSS) and two separate feeds, one for the 8- to 9-GHz band and one for the 30- to 40-GHz band. The major advantage of this configuration is that the feed design is simple. Two standard, wide-angle, corrugated feeds can easily be designed to cover each of the bands. Unfortunately, three major disadvantages exist as well. The first disadvantage is that the two feeds will demand two separate dewars or one very large dewar that houses both. An associated disadvantage is that there will be relatively large blockage due to the size of the FSS and feeds. The third disadvantage is that the FSS design will be rather difficult, requiring over both a wide bandwidth, up to 20 percent, and a wide range of angles of incidence, ± 42 deg. These three disadvantages were considered to be significant, and this approach was eliminated from further consideration.

The second configuration is based on the Jason II feed, which was designed by the Microwave Engineering Corporation.[3] In this particular design, the high-frequency band is fed into a corrugated horn in a conventional manner. The low-frequency band is injected through slots in the bottom of the corrugations at an appropriate location downstream. In this case, the corrugation depth must be chosen to provide the appropriate surface impedance in both bands. This may demand ring-loaded or dual-depth slots. The advantages of this feed design are that it is all metal with no dielectric elements and that matching the two bands is relatively straightforward. The two main disadvantages are the complicated corrugation design and the fact that to date the slot-coupled design has worked well only for linearly polarized applications. Some preliminary calculations were done on the corrugation design for this feed. The results were not favorable, particularly over the 20 percent bandwidth required in the 30- to 40-GHz band. In addition, the uncertainty of the design for circular polarization was a factor in its elimination from further consideration.

The third configuration that was studied is an all-metal coaxial design described by Johansson [4]. In this design, the feed is a coaxial structure where the low-frequency signals are carried in a coaxial guide in the TE_{11} coaxial mode while the high frequencies are carried by the hollow center conductor of the coaxial guide in the TE_{11} circular waveguide mode. Dual-depth corrugations are used to create symmetric radiation patterns in both bands. The main advantage of this design is its all-metal construction. This design was studied extensively, and two significant issues were encountered. The first serious issue involved the design of the dual-depth corrugations and operation over the 30- to 40-GHz bandwidth. The second concerned a significant mismatch at the throat of the horn in the lower-frequency band. Matching proved to be very difficult over the 8- to 8.8-GHz band. After a significant amount of design effort, this approach also was abandoned in favor of option four, described next.

The fourth, and chosen, configuration for the feed is similar to that described in Lee [5]. A similar design also is employed by the National Radio Astronomy Observatory (NRAO) at Green Bank, West Virginia, in an X-/S-band feed for radio astronomy. This feed is similar to that of the third configuration with the introduction of a dielectric rod element to control the radiation characteristics in the high-frequency band. This has the beneficial effect of reducing the blockage in the coaxial throat region of the horn. This in turn improves the return-loss characteristics in the low-frequency band. Introduction of the dielectric element also decouples the high-frequency band from the corrugations in the horn, allowing them to be

[3] Microwave Engineering Corporation, *Final Report on Development of 5 Frequency Feed for Jason II Antenna*, internal document, North Andover, Massachusetts, November 1999.

optimized for the low-frequency band only. In short, introduction of the dielectric rod decouples the low-frequency band design from the high-band design and simultaneously improves the low-frequency band match. The only disadvantages of this design are the possible loss introduced by the dielectric rod and the increased complexity of analyzing the dielectric loaded horn. The second disadvantage was mitigated through the use of an existing in-house computer code in the design process. The loss introduced by the rod was estimated and deemed acceptable for the present application. This design therefore was pursued and a final design was completed. The next section gives a brief description of the design tools used to develop the feed.

IV. Design Tools

Due to the complexity of this particular feed design, a number of different analysis tools were used in the design. Results produced by these various tools were combined as necessary using MATLAB scripts to cascade the various scattering parameters.

The corrugated horn and iris-loaded coaxial guide that make up the basic X-band radiator were analyzed as a single unit using JPL-developed mode-matching codes [6]. These programs were modified in order to accommodate the unusual groove design of the present horn. In the mode-matching analysis, the field in each subsection of the device is represented as a sum of forward- and backward-traveling or decaying waveguide modes. The amplitudes of these modes are determined by matching the electric and magnetic fields over each common waveguide aperture. This approach is very fast and accurate, requiring only a few seconds of central processing unit (CPU) time for each frequency point, modeling the entire horn and coaxial waveguide matching section. Although there is a dielectric rod present in the horn as well, it is ignored during this phase of the analysis/design. It is considered later in the finite-element analysis described next.

Due to the presence of the dielectric rod, mode matching is not applicable to the design of the 30- to 40-GHz portion of the feed. In this case, the finite-element method (FEM) was used to model the feed. An existing JPL code developed for FEM analysis of an arbitrary body of revolution (BOR) was used [7]. An exact modal expansion is used at the input port of the feed; finite elements are used to model the inhomogeneous portion of the feed; and an exact radiation boundary condition is used at the radiating aperture of the horn. All features of the horn are included in this model, including the external metal walls of the horn. Using the BOR representation is very efficient, converting the three-dimensional (3-D) geometry to two dimensions by taking advantage of the rotational symmetry of the component. Commercial finite-element tools, such as the one described next, do not have BOR capability and would require large amounts of CPU time and memory to compute results for this geometry. The FEM-BOR code provided results on a conventional workstation in a few minutes per frequency point for this problem. A typical result provided by this code is depicted in Fig. 1, showing a cross section of the feed including the excitation ports, corrugations, dielectric rod, and, in this case, a multi-layer spherical window. Although this analysis approach was used primarily in the 30- to 40-GHz band, the performance of the horn at 8 to 9 GHz also was computed with this code, taking into account the presence of the dielectric rod that was ignored in the initial mode-matching analysis described previously.

All components of the feed that could not be analyzed by mode matching or BOR techniques were analyzed using a commercial 3-D finite-element simulator, HFSS [8]. An example of a component that was analyzed in this manner is the coaxial turnstile junction depicted in Fig. 2. In all cases, any symmetry present in the device was used to reduce the simulation time; hence, only a 1/4 model of the turnstile junction is depicted in Fig. 2. The matching of these junctions was optimized using the 3-D modeler, although final bench tuning also proved necessary.

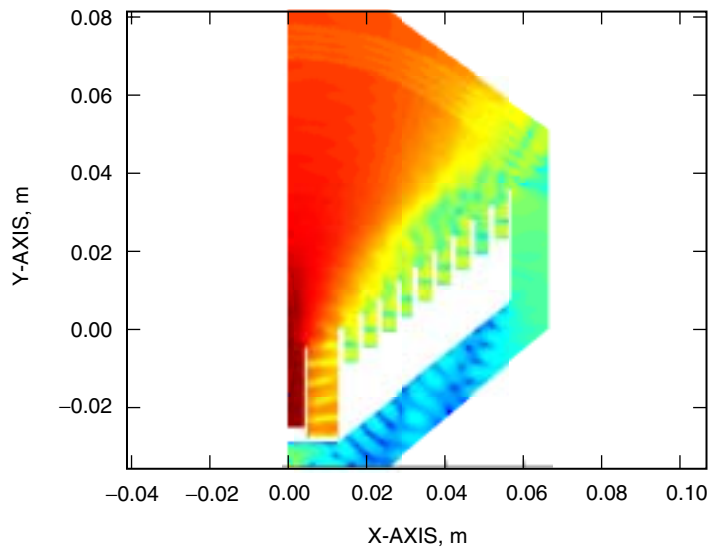

Fig. 1. Sample result from the finite-element body-of-revolution code.

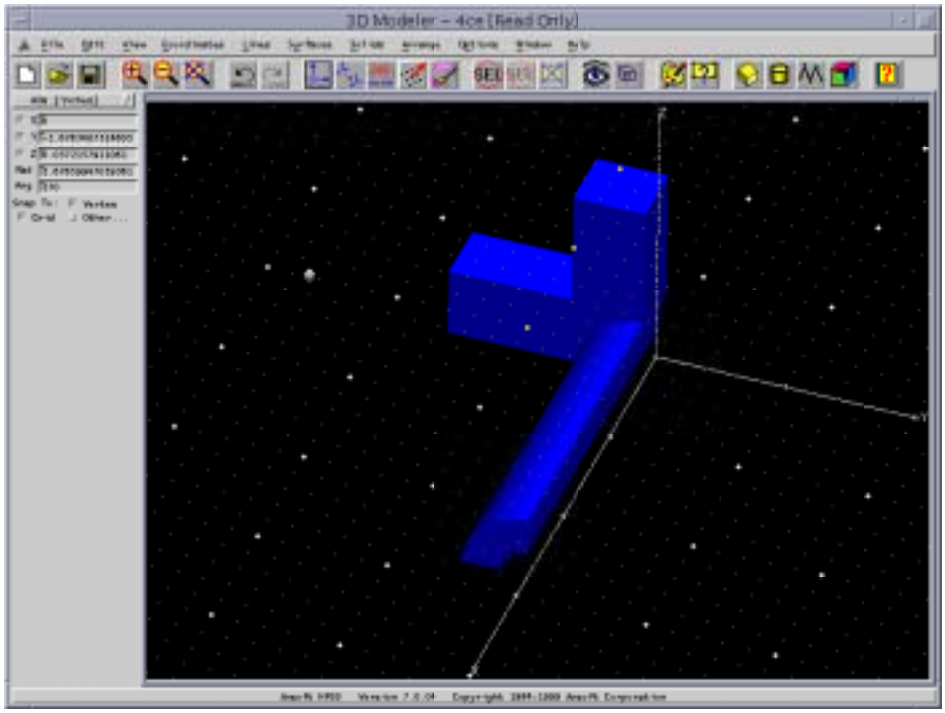

Fig. 2. Three-dimensional finite-element model of one of the turnstile junctions (1/4 model).

V. Final Design

A. Overview

In this section, the details of the final feed design will be described. Figure 3 shows a schematic of the dual-frequency feed, while Figs. 4 and 5 are photographs of the final prototype.

B. 8- to 9-GHz Band Components

The 8- to 9-GHz band of frequencies enters the horn through a commercial septum polarizer, catalog item AMC 1869 from the Atlantic Microwave Corporation (AMC) [9]. The input waveguide size is WR-112 while the square output dimension is 2.2606 cm (0.89 in.). Specifications call for ellipticity less than 0.8 dB and a voltage standing wave ratio (VSWR) less than 1.2:1 over a bandwidth of 8.0 to 8.8 GHz. The square waveguide then enters a square turnstile junction, where it exits in four orthogonal WR-112 waveguides. These guides then wrap around the 30- to 40-GHz output section and are recombined in a second turnstile junction. The common port of this turnstile junction is a coaxial waveguide operating in the TE_{11} coaxial mode. Both turnstile junctions were matched by adjusting circular steps at the base of

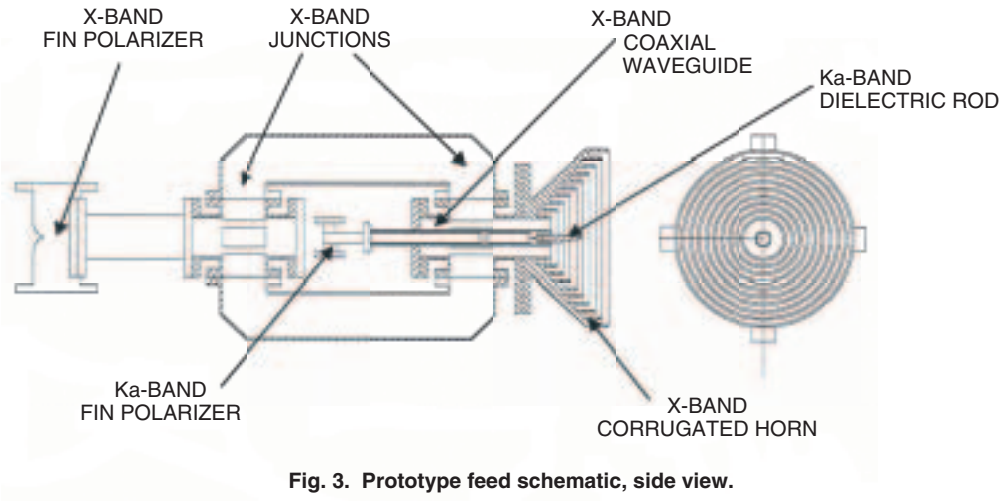

Fig. 3. Prototype feed schematic, side view.

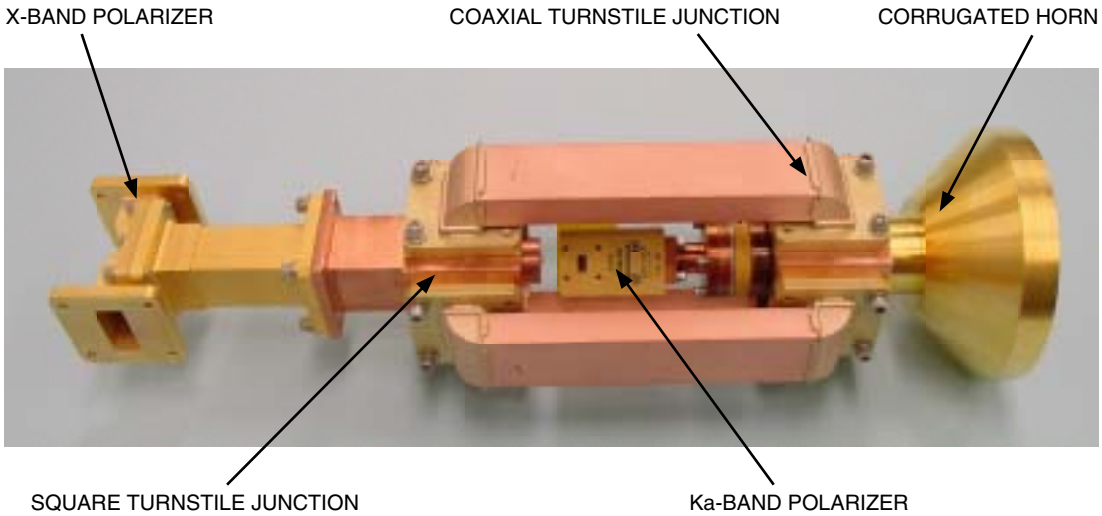

Fig. 4. Prototype feed, side view.

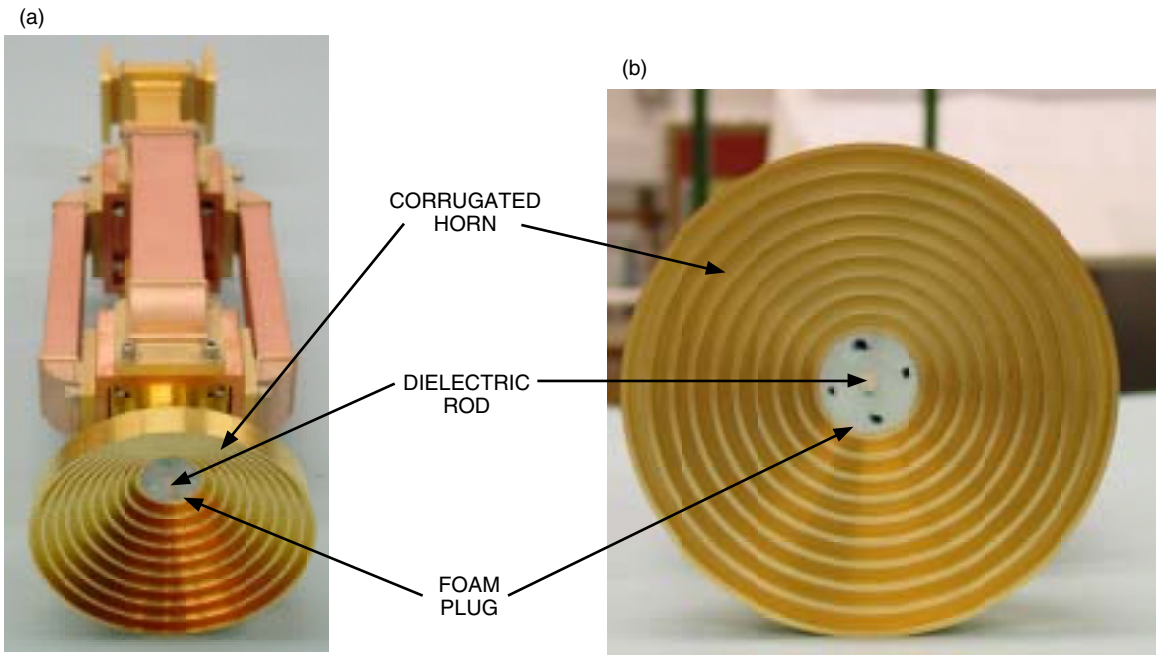

Fig. 5. Prototype feed: (a) top view and (b) front view.

the turnstile, initially through analysis using HFSS and with final adjustments done experimentally. The outer diameter of this coaxial guide is 2.54 cm (1.0 in.), and the inner diameter that also forms the outer wall of the 30- to 40-GHz circular waveguide is 1.016 cm (0.4 in.). The coaxial guide then terminates in the throat of the horn. A single thick iris is used to match the horn aperture. Coaxial mode matching was used to determine the appropriate iris dimensions and position. The initial flare angle of the horn was determined using a Gaussian beam design, and final dimensions were determined using a JPL-developed mode-matching program. The resulting corrugation depth was 0.88646 cm (0.349 in.); the corrugation width was 0.3175 cm (0.125 in.); and the period was 0.950 cm (0.374 in.). Although the initial design of the 8- to 9-GHz portion of the horn was designed ignoring the presence of the 30- to 40-GHz dielectric rod, final simulations were conducted using the FEM-BOR code. No modifications to the horn portion of the design were required, and small corrections to the matching iris design were determined experimentally.

C. 30- to 40-GHz Band Components

The 30- to 40-GHz signals enter the horn through a second septum polarizer—in this case, a custom-designed component from AMC. Input waveguides are WR-28, with an output in 0.5842-cm (0.242-in.)-diameter circular waveguide. The polarizer VSWR is specified to be less than 1.2:1 over the 31.8- to 38.0-GHz band, while ellipticity is specified over only the DSN receive and future HEDS bands, ellipticity $<$0.75 dB at 31.8 to 32.3 GHz and 37 to 38 GHz. At the time of this article, a polarizer has not been produced that meets all of the requested specifications, and back-up approaches currently are being considered.

The inner diameter (ID) of the circular waveguide then is tapered to 0.8636 cm (0.340 in.), and this waveguide is extended through the center conductor of the 8- to 9-GHz coaxial waveguide to the throat of the horn. The signal then enters a tapered Teflon rod where it is radiated into free space. The key dimensions of the rod are shown in Fig. 6. The input taper provides a natural match to the waveguide while an output taper helps release the radiation to free space. Since the dielectric rod diameter is less than the circular waveguide diameter, a foam plug is used for support; see Fig. 5. Efforts to extend the dielectric rod diameter to that of the waveguide, forming a snug fit, were unsuccessful. The dimensions and axial location of the rod were optimized to produce the desired pattern shape, input match, and phase

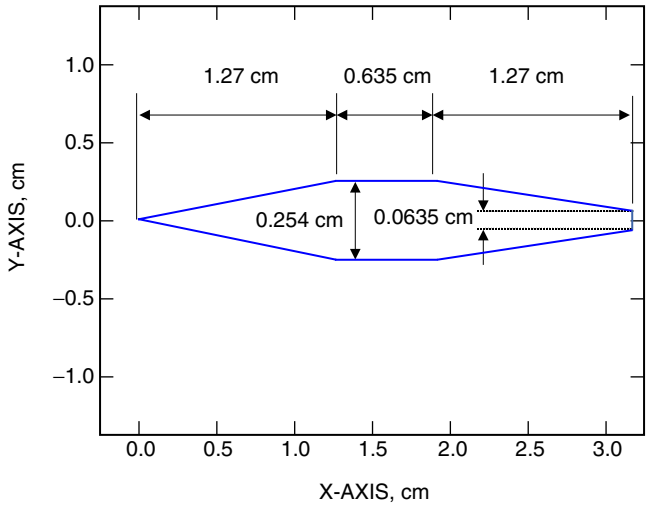

Fig. 6. Dielectric rod dimensions.

center location. Calculations were carried out using the FEM-BOR code. Initially the rod performance was optimized without the corrugated horn present in order to improve calculation speed. Only small modifications to the rod design were required after the corrugated horn was added to the BOR model.

D. Window

The window for the feed must produce low reflection and low loss in both bands, have sufficient strength to withstand atmospheric pressure, and provide thermal insulation as well. This is a significant challenge. The present window design is a three-layer design, with a 0.08-mm Kapton layer for strength, backed by a 25-mm polystyrene layer for additional strength and thermal insulation, with a 0.38-mm Teflon over-layer to protect the Kapton, which will lose strength after long periods of exposure to the Sun. The window adds less than 1 K of noise temperature to the system in each band. Although the window design is satisfactory for the breadboard array, it is recognized that a more robust design is required for the final array. This is discussed further in Section VIII. The feed-horn window is described in more detail in [10].

VI. Measured Performance

A. 8- to 9-GHz Band

The return loss of the prototype horn depicted in Figs. 4 and 5 was measured using an HP 8510 network analyzer, and these results are depicted in Fig. 7. The measured return loss is approximately −25 dB over the 8.0- to 8.8-GHz band, and it rises slightly from 8.9 to 9.0 GHz. With the septum polarizer connected to the feed, reflections from any point past the polarizer have a reversed sense of polarization relative to the incident wave. These signals then appear at the opposite port of the polarizer upon reflection. A measurement of this isolation term is depicted in Fig. 8. The isolation is approximately −20 dB across the 8.0- to 8.8-GHz band, rising above −20 dB from 8.85 to 9.0 GHz.

The radiation patterns of the feed also were measured on the Mesa Antenna Range. Radiation patterns at 8.0, 8.4, and 8.8 GHz are depicted in Figs. 9 through 11. The targeted relative gain value, −12 dB at ±42 deg, is matched quite closely in all figures. As can be seen, the radiation pattern of the feed is slowly varying, very symmetric, and well behaved across the entire frequency band of interest.

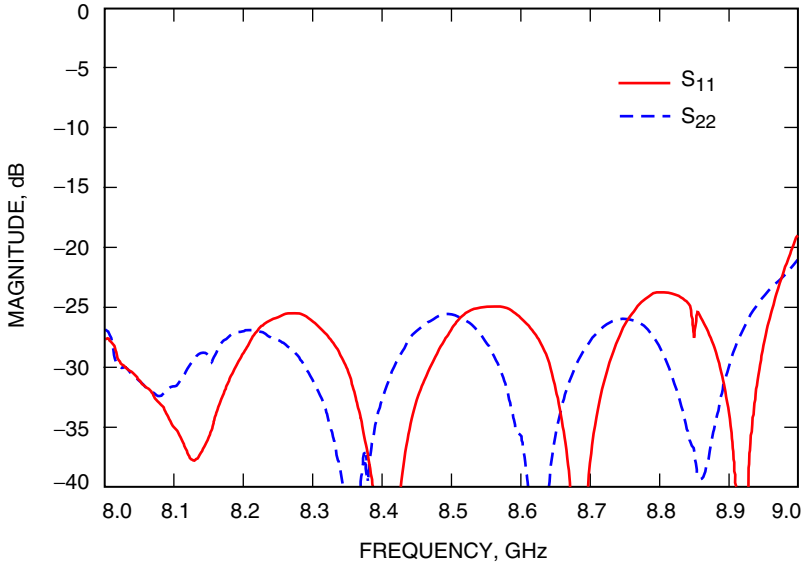

Fig. 7. Measured return loss in the 8- to 9-GHz band.

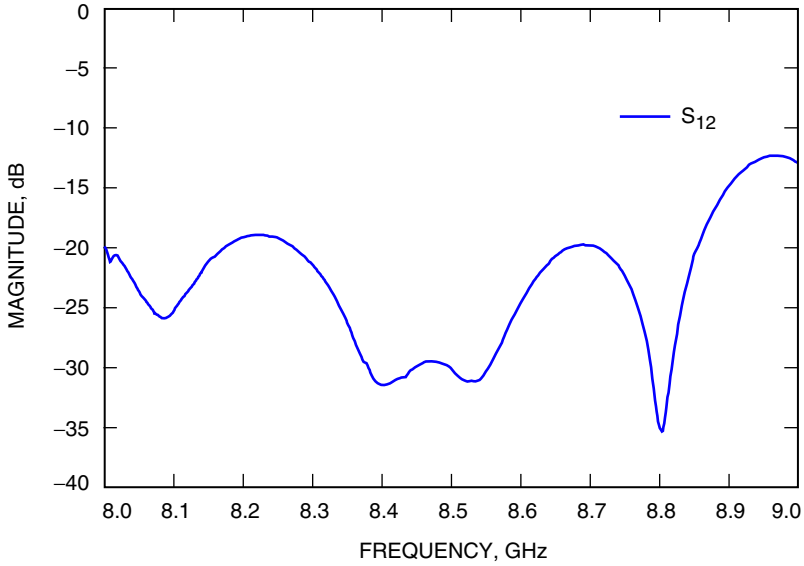

Fig. 8. Measured isolation in the 8- to 9-GHz band.

B. 30- to 40-GHz Band

The measured return loss of the feed in the 30- to 40-GHz band is shown in Fig. 12. Linearly polarized results were obtained by measuring through the temporary WR-28-to-circular-waveguide transition, prior to arrival of the septum polarizer. The measured return loss is approximately −25 dB across the entire 30- to 40-GHz band.

Figures 13 through 17 present the measured feed radiation patterns from 30 to 38 GHz at 2-GHz intervals. The target illumination is nearly met at an operating frequency of 30 GHz, and a gradual narrowing of the beam across the 30- to 40-GHz band occurs. A design decision was made to accept this beam narrowing in order to obtain a more stable phase-center location across the 30- to 40-GHz band. A future iteration of the dielectric rod design could be undertaken in order to improve both the beam-width

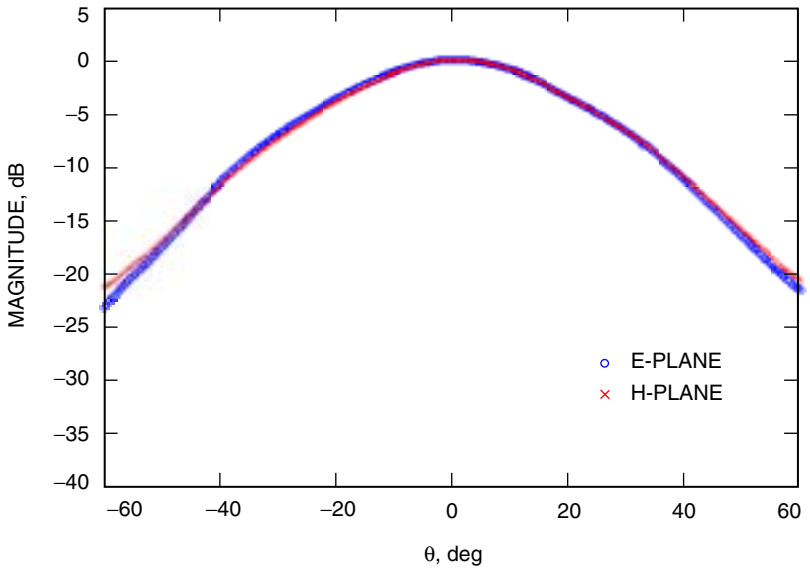

Fig. 9. Feed radiation pattern at 8.0 GHz.

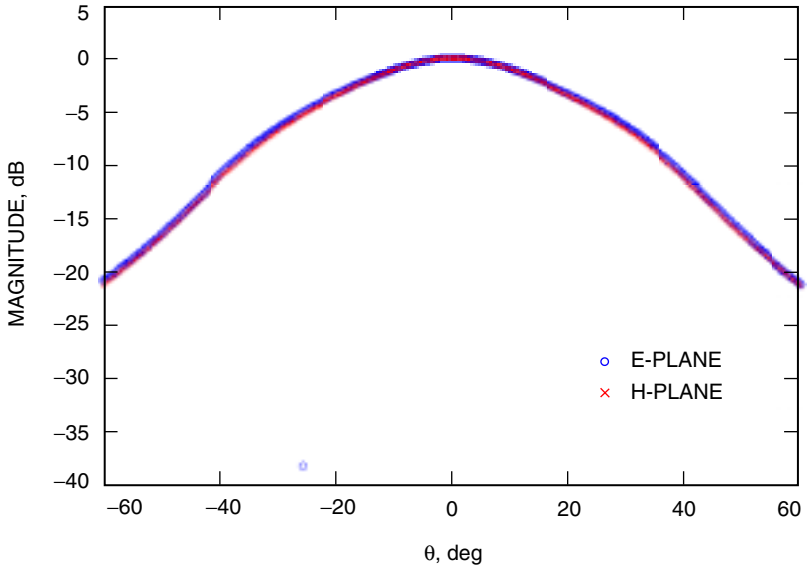

Fig. 10. Feed radiation pattern at 8.4 GHz.

variation and the E-/H-plane symmetry of the feed in this band. Fortunately, the beam narrowing has only a slight impact on antenna efficiency when this feed is used on the dual-shaped reflector antenna designed for the DSN large array. A summary of these efficiency calculations is presented in the next section.

VII. Computed Performance on the 6-Meter Shaped Dual-Reflector Antenna

For completeness, Figs. 18 and 19 depict the computed value of the antenna gain-to-system noise temperature ratio (G/T) for the feed used in conjunction with a 6-meter shaped dual-reflector antenna. The details of the antenna design and associated performance are given in [11]. The reflector shaping was performed using computed feed radiation patterns, and upon completion of the prototype, measured

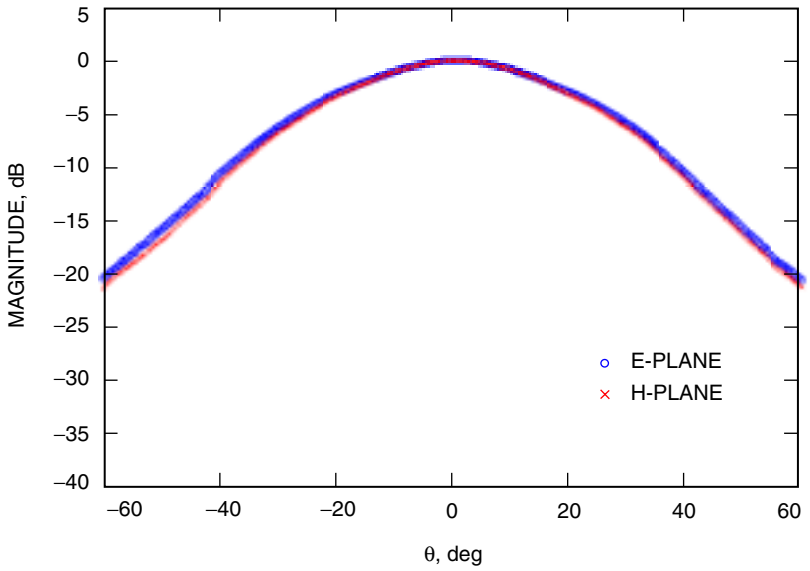

Fig. 11. Feed radiation pattern at 8.8 GHz.

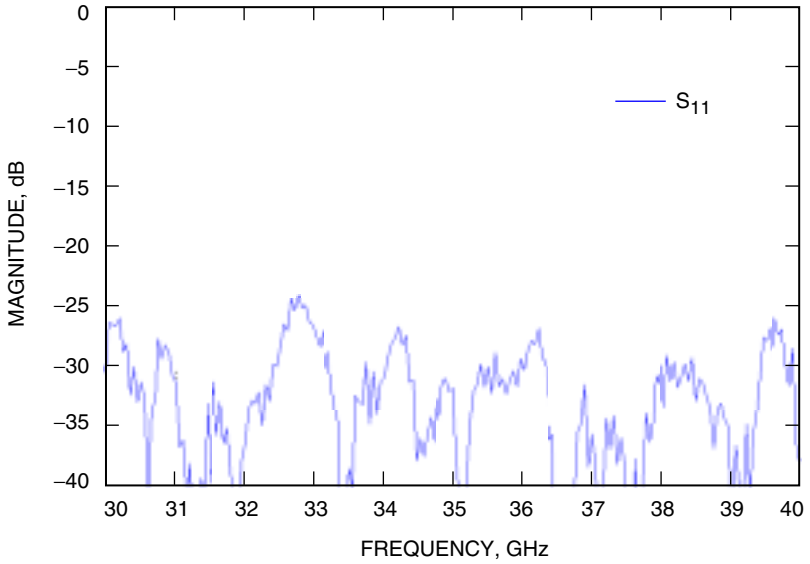

Fig. 12. Measured return loss in the 30- to 40-GHz band.

patterns were used to compute the true antenna performance. Figure 18 shows the computed G/T rising from 40.5 dB/K at 8.0 GHz to 41.5 dB/K at 9.0 GHz using the theoretical feed radiation patterns. G/T computed within the DSN band from 8.4 to 8.5 GHz using the measured feed patterns actually exceeds these original predictions by a few tenths of a dB. As was mentioned earlier, the feed patterns in the 8- to 9-GHz band are very slowly varying and well behaved. We expect excellent agreement between the computed values for G/T in the 8- to 9-GHz band and the values that will later be measured experimentally. Figure 19 shows G/T increasing from 48.5 dB/K at 30.0 GHz to 50.75 dB/K at 40.0 GHz using the predicted feed radiation patterns. These results are nearly achieved using the measured feed patterns, with a roll-off of a few tenths of a dB at the upper end of the band due to slightly more narrowing of the feed radiation than originally predicted. It should be noted that the results shown in Figs. 18 and 19 were achieved by optimizing the axial position of the feed on the reflector antenna,

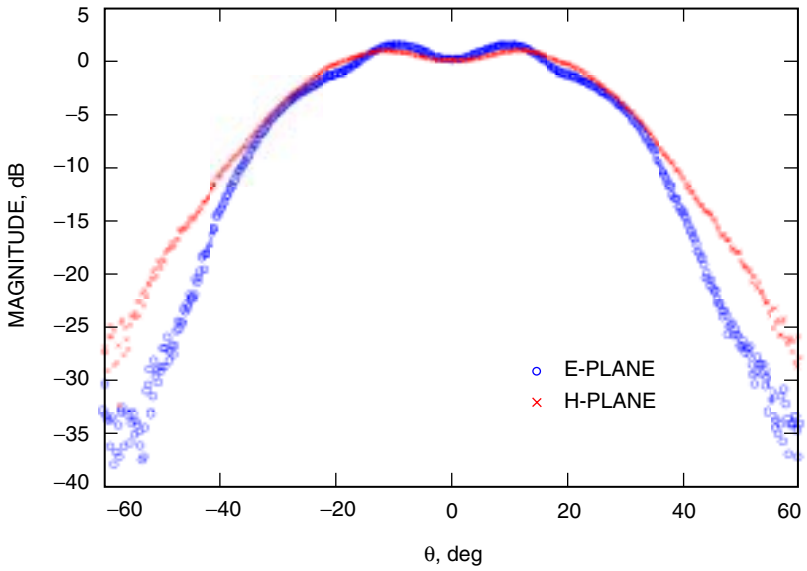

Fig. 13. Feed radiation pattern at 30.0 GHz.

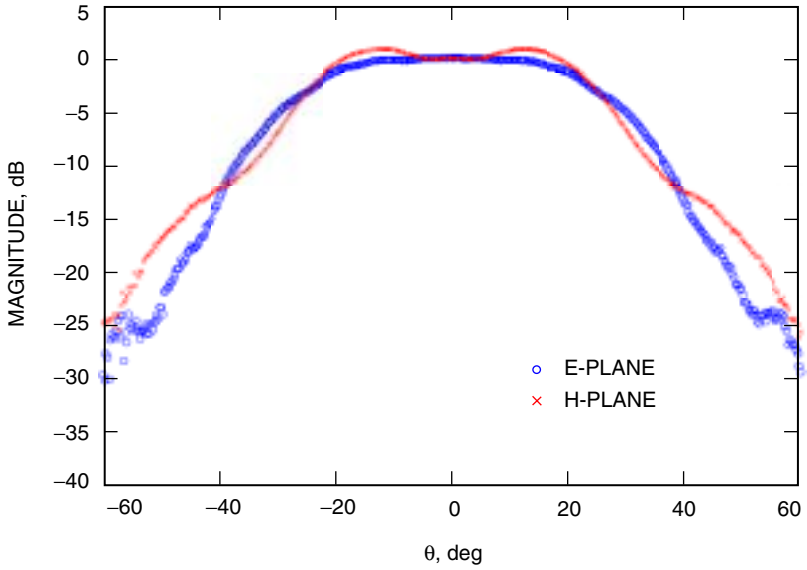

Fig. 14. Feed radiation pattern at 32.0 GHz.

balancing the slight difference in phase center between the two bands of operation. More details about this optimization process can be found in [11].

VIII. Conclusions and Future Work

Three additional copies of the feed described in this article are currently in fabrication. These feeds will be used in conjunction with three 6-meter dual-shaped reflector antennas to form the breadboard DSN array. This prototype will be used to determine performance and cost estimates for the final array and to learn more about the practical aspects of building and operating such an array.

Prior to fabrication of a large number of these feeds for the DSN large array, a few small but important modifications/improvements to the design should be investigated. The first item that should be in-

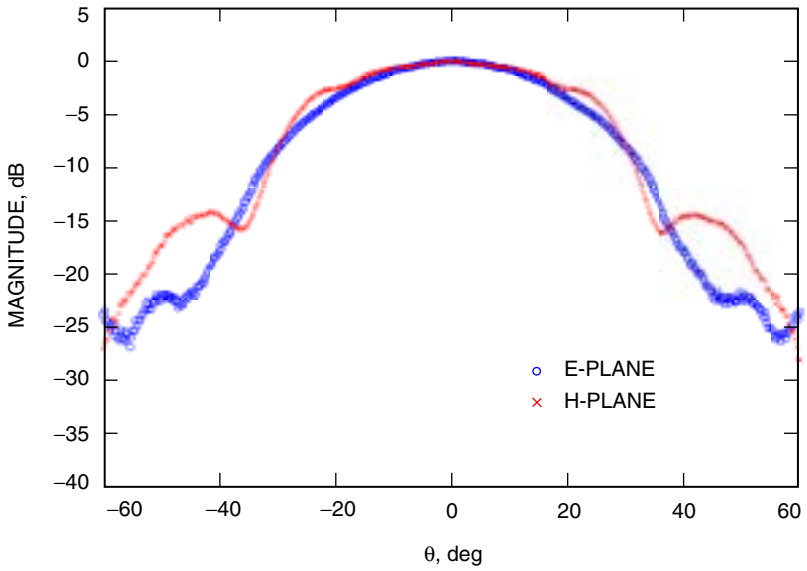

Fig. 15. Feed radiation pattern at 34.0 GHz.

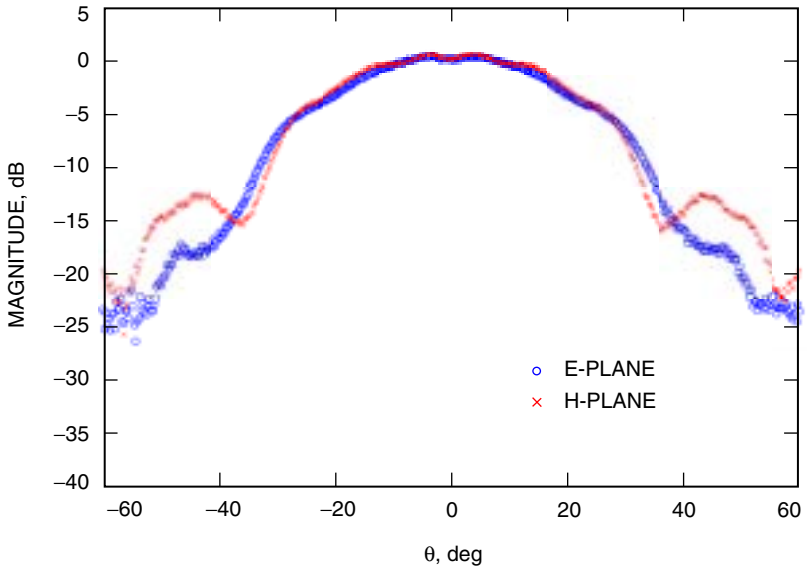

Fig. 16. Feed radiation pattern at 36.0 GHz.

vestigated is the mounting approach for the dielectric rod in the feed. The dielectric plug used in the present design has the disadvantage that it is non-rigid, making it difficult to accurately position the rod in its optimal location. Several proposed solutions to this problem should be investigated. These include the use of an alternative foam plug with more rigidity or the use of a dielectric spider web structure, integral with the rod, to position it axially along the centerline of the 30- to 40-GHz circular waveguide.

The second area that should be investigated is a more robust window design. Although the three-layer approach employed in the prototype has high performance, there are some concerns regarding its ultimate lifetime/survivability in an operational environment. Failure of the window will result in significant maintenance and downtime for the antenna involved. Preliminary calculations indicate that a three-layer design based on a Rexolite center layer is feasible. The remaining design question involves the

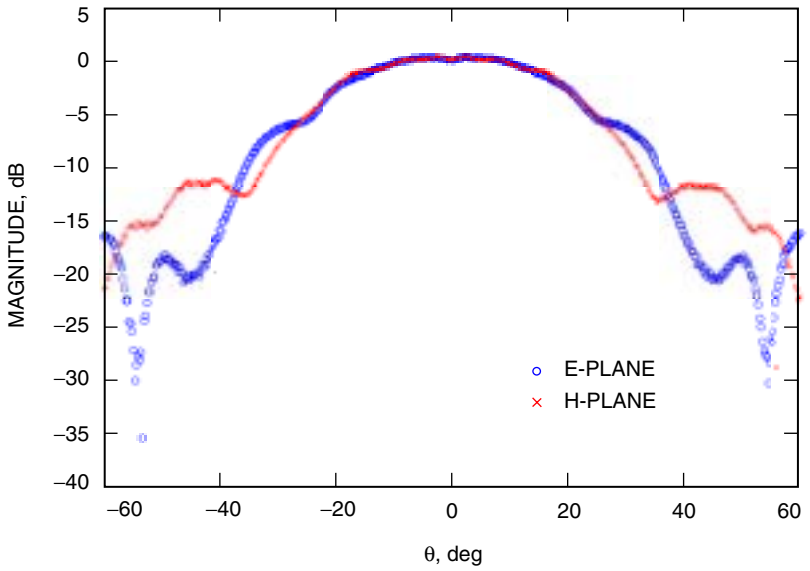

Fig. 17. Feed radiation pattern at 38.0 GHz.

realization of the matching layers, whether these layers should indeed be fabricated as homogeneous layers or whether creating an "effective" dielectric using holes or grooves in the Rexolite is a more practical design.

Finally, it may be possible to improve the 30- to 40-GHz radiation patterns slightly through another iteration of the dielectric rod design. This design iteration should be pursued if the measurements and/or calculations indicate that the 30- to 40-GHz antenna efficiency is a driving factor on the cost of the overall DSN large array.

As of the writing of this article, the noise temperature performance of the prototype feed has not been characterized. Preliminary tests have encountered several difficulties stemming from the angular width of the radiation pattern of the feed and the large bandwidth of operation. The large angular beam width has made it necessary to construct a special noise shield to prevent excessive noise pickup from structures surrounding the feed in the test area. The large operational bandwidth, 8 to 9 GHz and 30 to 40 GHz, has rendered standard DSN low-noise amplifiers insufficient for characterization of the feed. At present we are waiting for delivery of the first wide-band monolithic microwave integrated circuit (MMIC) amplifiers. Upon delivery these amplifiers will be integrated with the feed and cryogenic system, and noise temperature measurements will commence. A future article will discuss the results of these upcoming measurements.

Acknowledgments

In addition to the authors, several other individuals made important contributions to the development of this feed. The authors would like to acknowledge Jose Fernandez and Wesley Pickens for their efforts in measuring both the scattering parameters and radiation patterns of the feed, Manuel Esquivel for his help in the design of the dielectric rod element, and finally Larry Epp and Gilbert Chinn for their help in resurrecting the FEM-BOR computer code for this design task.

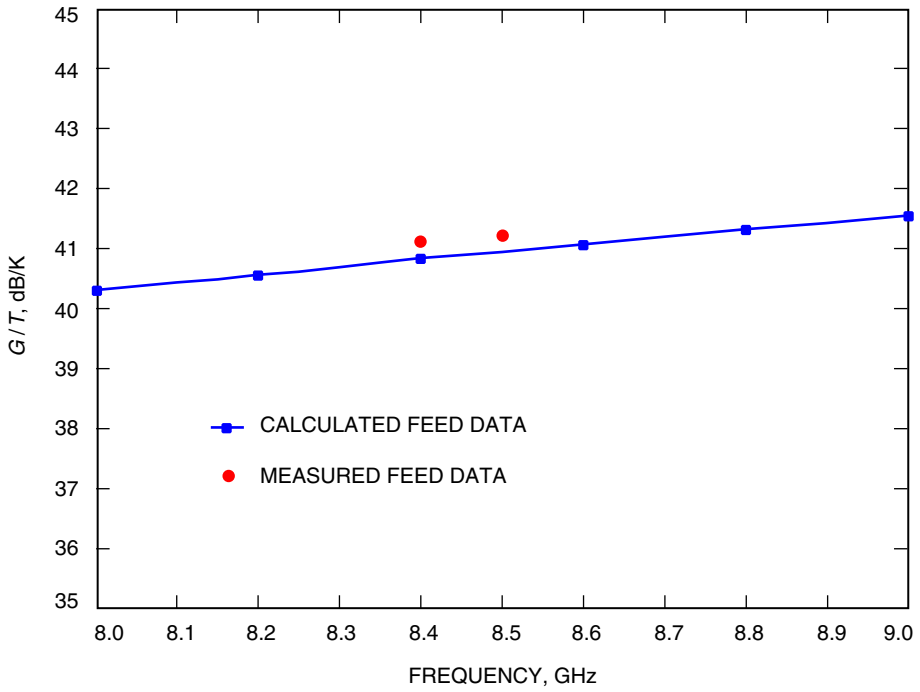

Fig. 18. Computed antenna efficiency in the 8- to 9-GHz band.

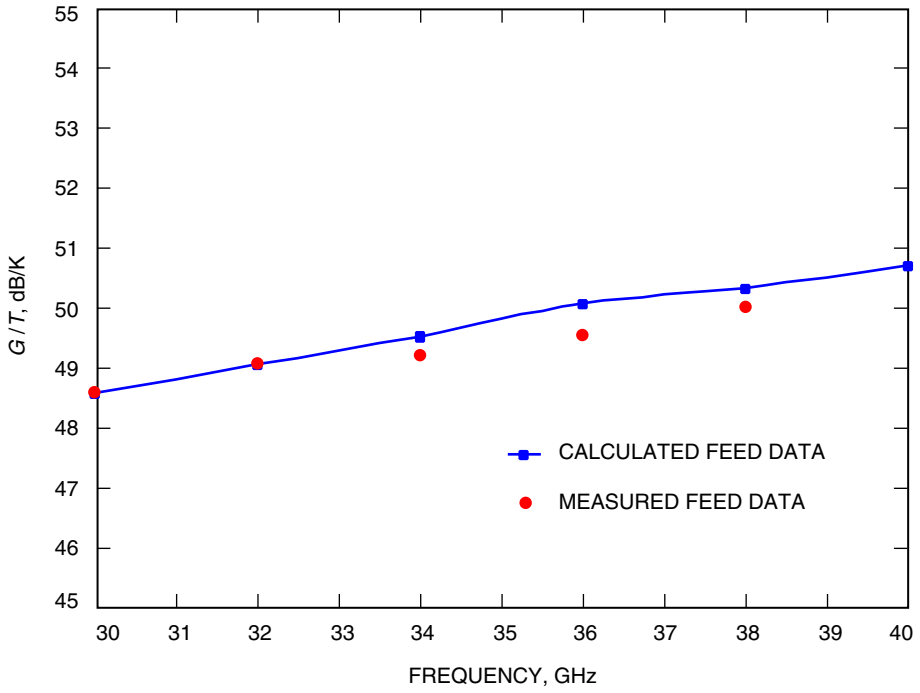

Fig. 19. Computed antenna efficiency in the 30- to 40-GHz band.

References

[1] M. S. Gatti, "The Deep Space Network Large Array," AIAA Space 2003 Conference, Long Beach, California, September 23–25, 2003.

[2] http://www.skatelescope.org/

[3] G. E. Moore, "Cramming More Components Onto Integrated Circuits," *Electronics*, vol. 38, no. 8, pp. 114–117, April 1965.

[4] M. Johansson and P. S. Kildal, "Coaxially Fed Dual-Frequency Horn for Offset Parabolic Reflector," *1995 IEEE Int. Antennas Symposium Digest*, vol. 33, pp. 1158–1161, June 1995.

[5] J. C. Lee, "A Compact Q/K-Band Dual Frequency Feed Horn," *IEEE Transactions on Antennas and Propagation*, vol. AP-32, no. 10, pp. 1108–1111, October 1984.

[6] D. J. Hoppe, "Modal Analysis Applied to Circular, Rectangular, and Coaxial Waveguides," *The Telecommunications and Data Acquisition Progress Report 42-95, July–September 1988*, Jet Propulsion Laboratory, Pasadena, California, pp. 89–96, November 15, 1988.
http://tmo.jpl.nasa.gov/tmo/progress_report/42-95/95I.PDF

[7] G. C. Chinn, L. W. Epp, and D. J. Hoppe, "A Hybrid Finite-Element Method for Axisymmetric Waveguide-Fed Horns," *IEEE Transactions on Antennas and Propagation*, vol. AP-44, no. 3, pp. 280–285, March 1996.

[8] http://www.ansoft.com/products/hf/hfss/

[9] http://www.atlanticmicrowave.com/

[10] M. J. Britcliffe, T. R. Hanson, and M. M. Franco, "Cryogenic Design of the Deep Space Network Large Array Low-Noise Amplifier System," *The Interplanetary Network Progress Report*, vol. 42-157, Jet Propulsion Laboratory, Pasadena, California, pp. 1–13, May 15, 2004.
http://ipnpr.jpl.nasa.gov/progress_report/42-157/157C.pdf

[11] W. A. Imbriale and R. Abraham, "Radio Frequency Optics Design of the Deep Space Network Large Array 6-Meter Breadboard Antenna," *The Interplanetary Network Progress Report*, vol. 42-157, Jet Propulsion Laboratory, Pasadena, California, pp. 1–8, May 15, 2004.
http://ipnpr.jpl.nasa.gov/progress_report/42-157/157E.pdf